Supporting Information

**Intercalating cobalt cation to Co_9S_8 interlayer for highly efficient and stable electrocatalytic hydrogen evolution**

Bin Tian[a], Wojciech Kolodziejczyk[a], Julia Saloni[a], Pohlee Cheah[a], Jing Qu[a], Fengxiang Han[a], Dongmei Cao[b], Xianchun Zhu[a], Yongfeng Zhao[a, *]

[a]Department of Chemistry, Physics and Atmospheric Science, Jackson State University, Jackson, MS 39217, USA

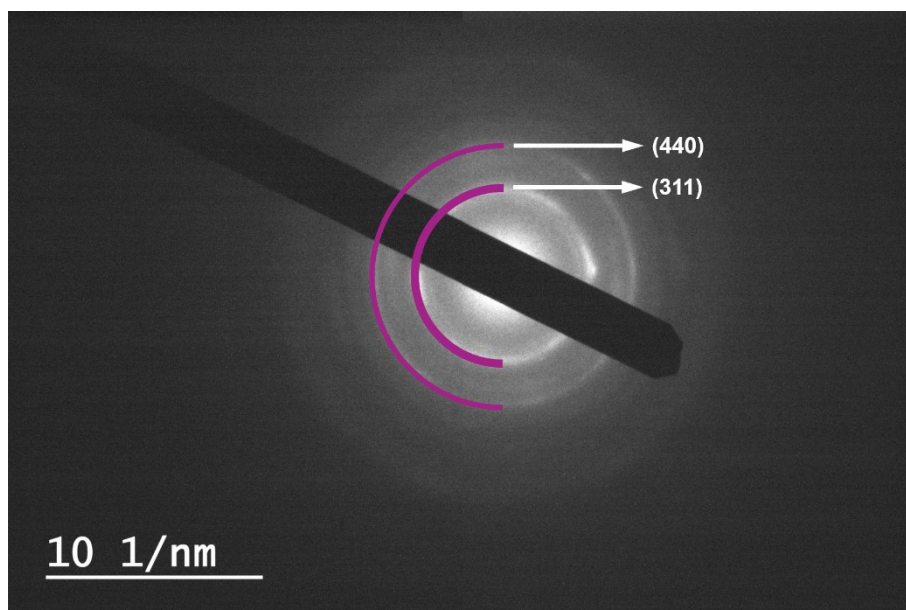[b]Material Characterization Center, Louisiana State University, Baton Rouge, LA 70803, USA

Correspondence should be addressed to Yongfeng Zhao: yongfeng.zhao@jsums.edu
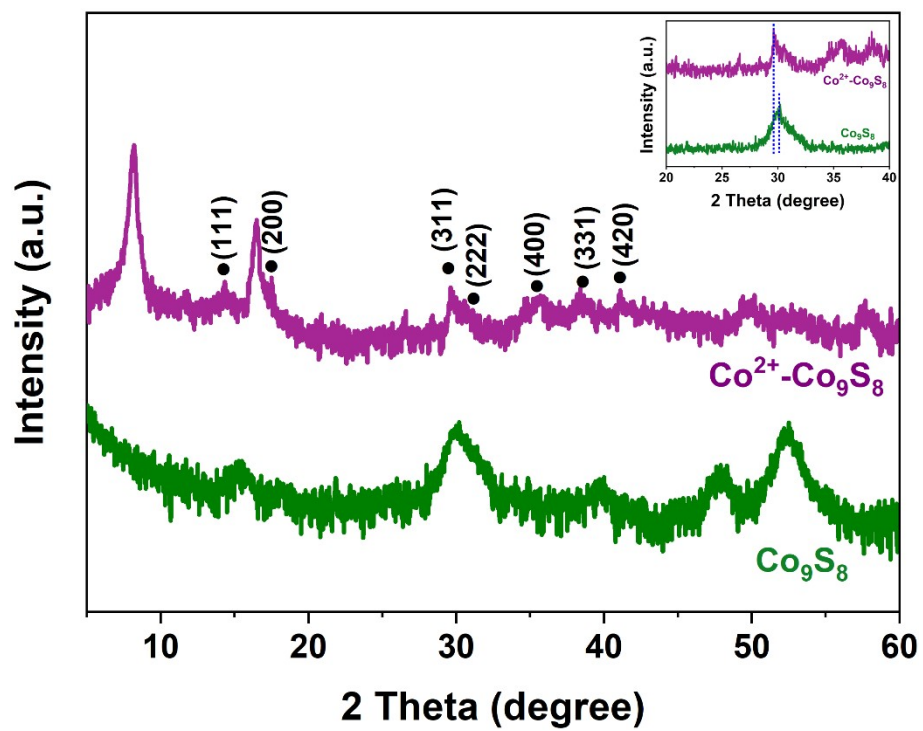
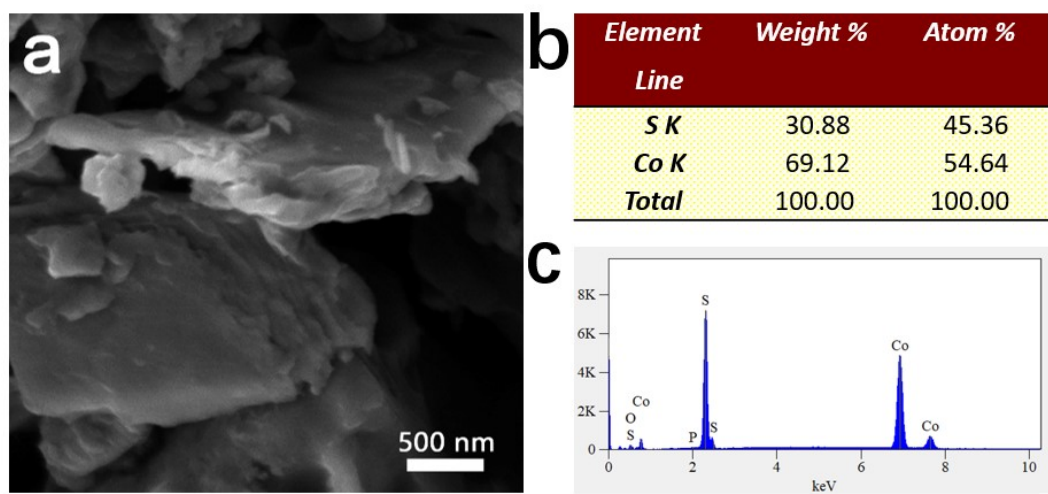**Figure S1.** XRD patterns of pure Co_9S_8 and Co^{2+}-Co_9S_8, the inset is the enlarged peaks in the range from 20 to 40°.
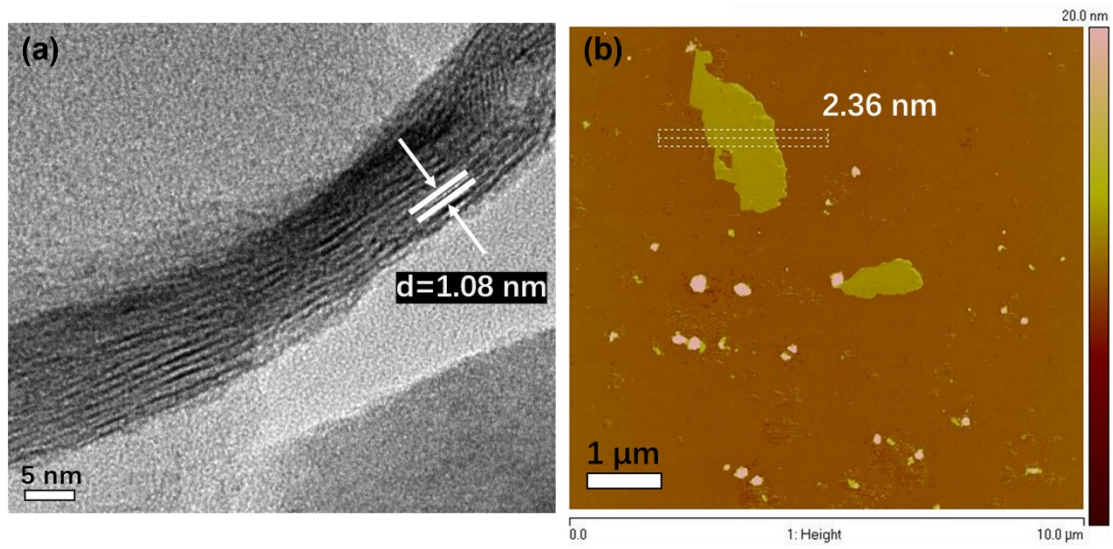
Figure S2. (a) The HRTEM image of Co^{2+}-Co_9S_8 and (b) AFM image of exfoliated Co^{2+}-Co_9S_8 sample.

Figure S3. The TEM selected area electron diffraction of Co^{2+}-Co_9S_8 catalysts.

Figure S4. (a) The SEM image of Co^{2+}-Co_9S_8. (b) and (c) The SEM EDS elemental analysis of Co^{2+}-Co_9S_8.
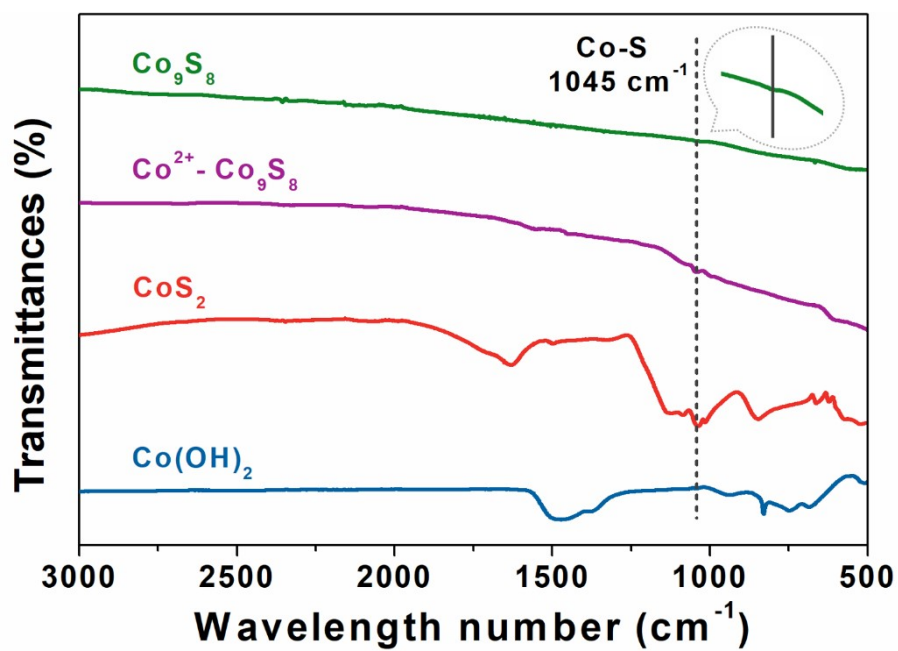
Figure S5. The FT-IR spectra of $Co(OH)_2$, CoS_2, pure Co_9S_8 and Co^{2+}-Co_9S_8
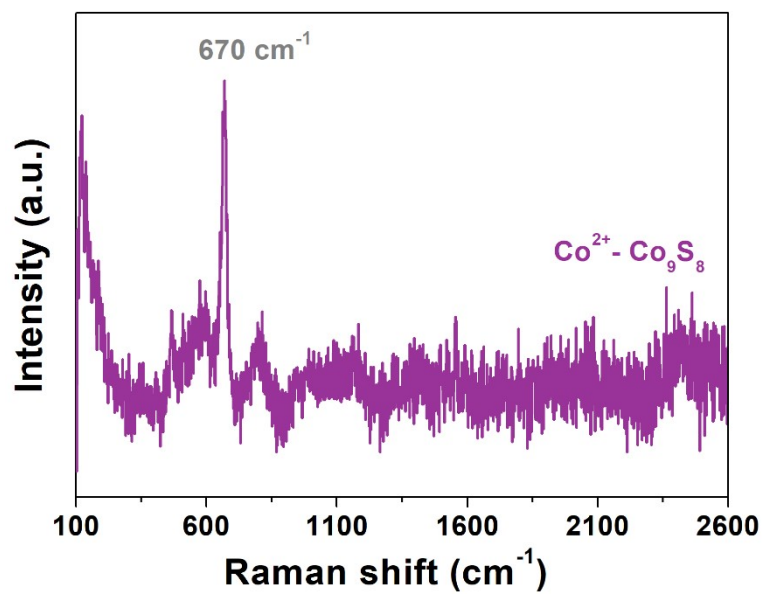
catalysts.

Figure S6. The Raman spectrum of Co^{2+}-Co_9S_8 sample, the excited wavelength is 532 nm.
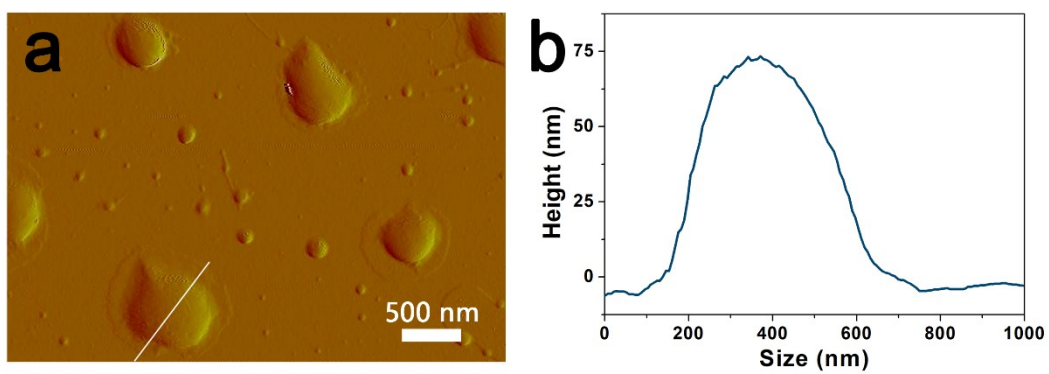
Figure S7. (a) The AFM image of Co^{2+}-Co_9S_8, (b) the corresponding size value.
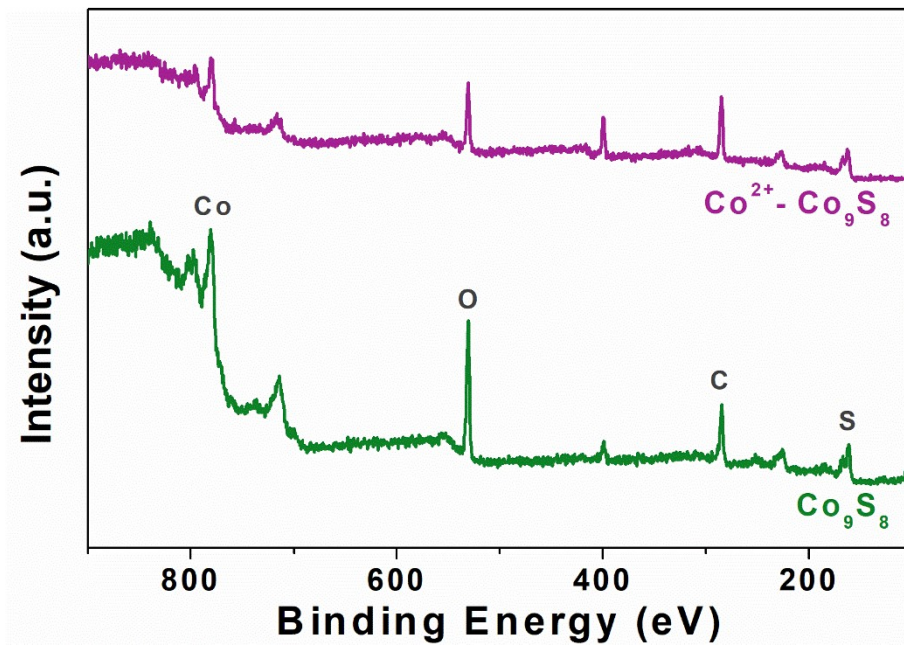
Figure S8. The XPS survey spectra of Co_9S_8 and Co^{2+}-Co_9S_8 catalysts.
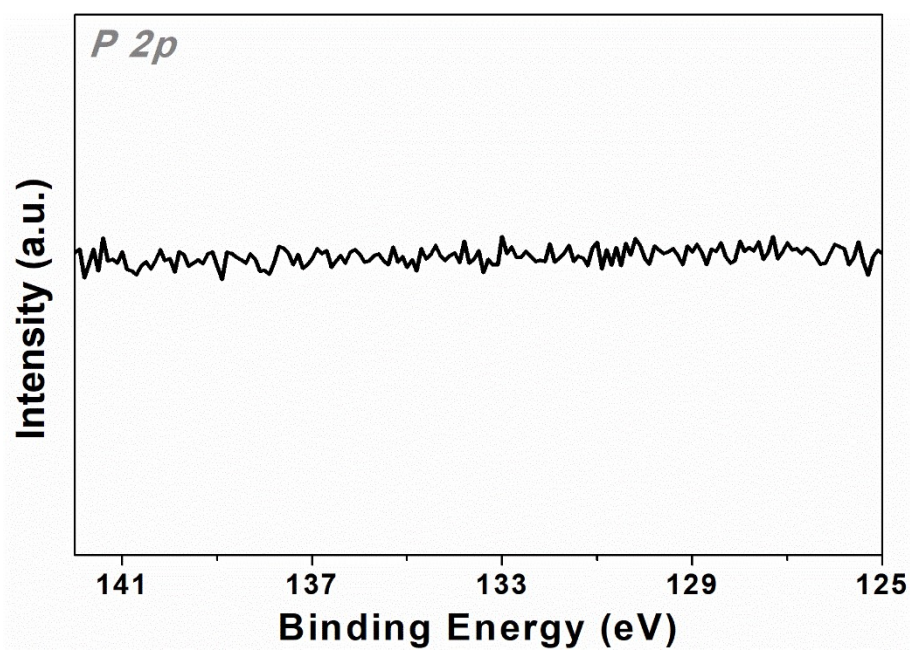
Figure S9. The XPS P $2p$ spectra of Co^{2+}-Co_9S_8 catalysts.
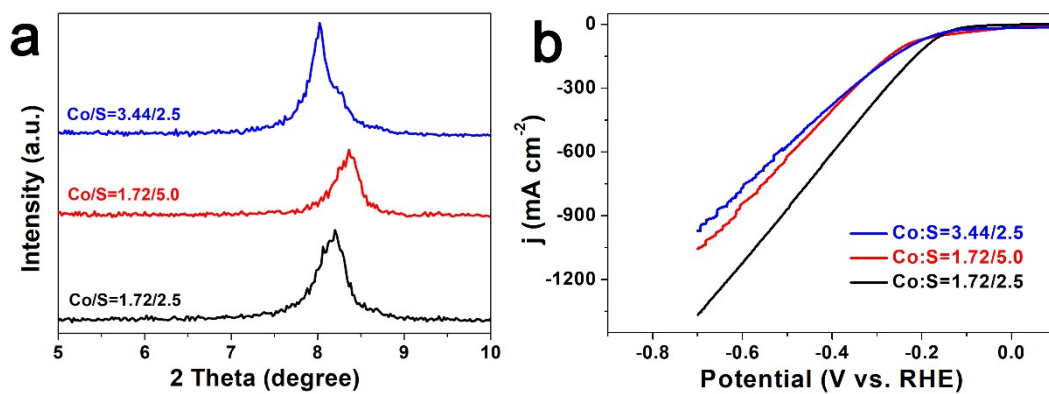
Figure S10. (a) The XRD patterns of Co^{2+}-Co_9S_8 samples with different amount of starting materials. (b) The polarization curves of Co^{2+}-Co_9S_8 catalysts different amount of starting materials.
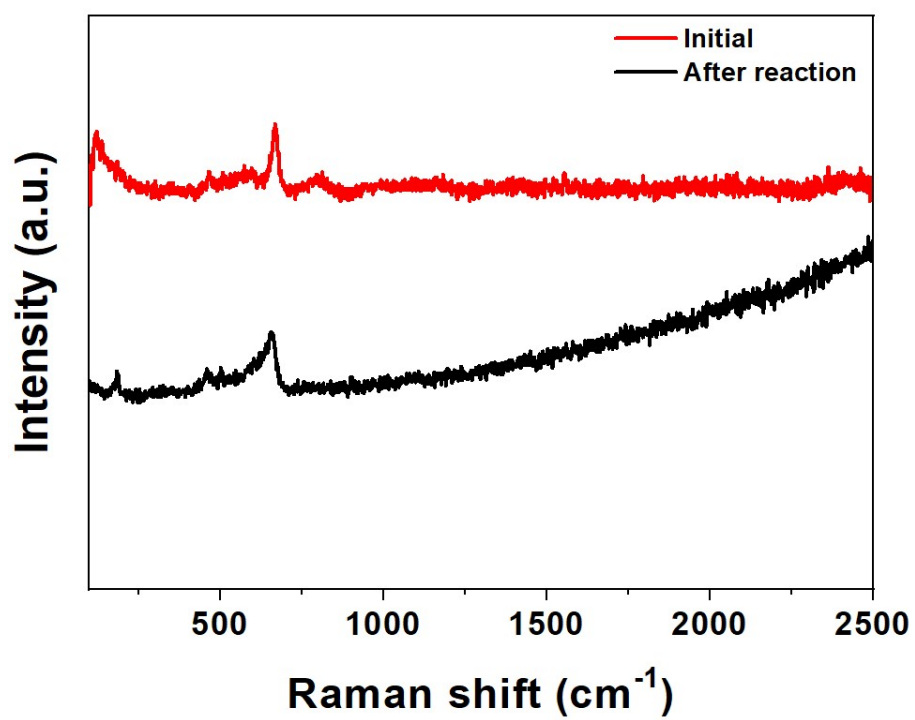
Figure S11. The Raman spectra of Co^{2+}-Co_9S_8 catalyst of initial and after reaction.
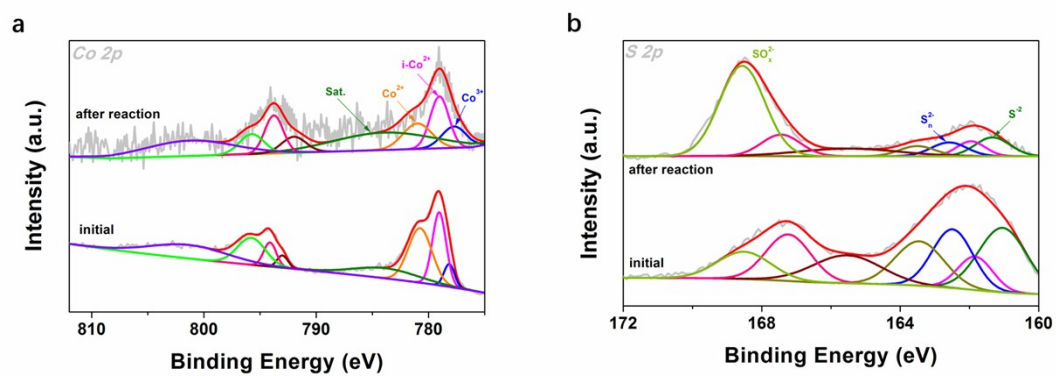
Figure S12. The comparison of high-resolution XPS spectra, including (a) Co *2p* and (b) S *2p* spectra between initial and after reaction of Co^{2+}-Co_9S_8 catalyst.
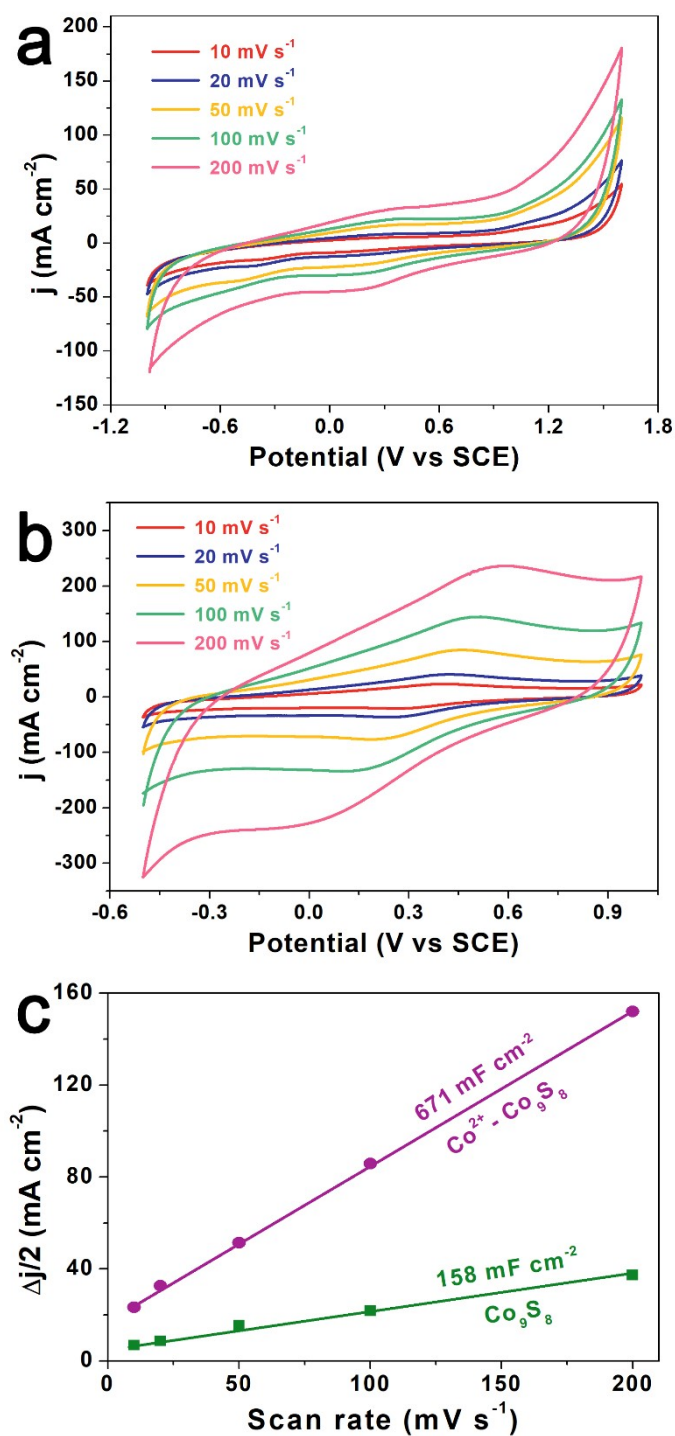
Figure S13. Electrochemical double-layer capacitance measurements. (a) and (b) Electrochemical cyclic voltammogram of as-grown catalysts at different potential scanning rates. The scan rates are 10, 20, 50, 100 and 200 mV s^{-1}. (c) Linear fitting of the capacitive currents of the catalysts *vs.* scan rates.
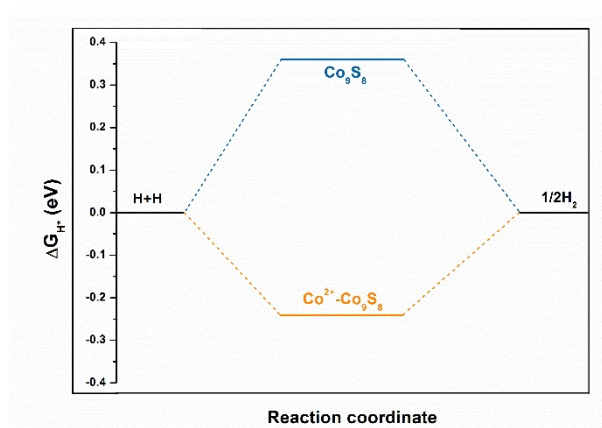
Figure S14. The calculated free-energy diagram for HER based on the pure Co_9S_8 and Co^{2+}-Co_9S_8 systems.

Table S1. The electrocatalytic HER performance comparison between our work and other literatures.

System	Condition (H_2SO_4)	Loading amount ($mg\ cm^{-2}$)	$\eta_{j\ =\ 10\ mA\ cm^{-2}}$ (mV vs. RHE)	Tafel Slop ($mV\ dec^{-1}$)	Ref.
Co_9S_8/NSG-220	0.5 M	0.38	-247	97	S1
Co_9S_8@MoS_2/CNFs	0.5 M	0.21	-190	110	S2
NSCDs/CoS	0.5 M	0.25	-265	56	S3
CoS_2/RGO-CNT	0.5 M	1.15	-142	51	S4
CoMoNiS-NF-31	0.5 M	1.86	-103	55	S5
Co_9S_8/NC@MoS_2	0.5 M	0.28	-117	68.8	S6
NiS-Ni_9S_8-NiSe-NR	0.5 M	0.25	-120	85.2	S7
$Ni_{43}Au_{57}$ nanoparticles/carb	0.5 M	0.20	-200	43	S8
HNDCM-Co/CoP	0.5 M	N/A	-138	66	S9
CoP/NPC/TF	0.5 M	N/A	-91	54	S10
Co^{2+}-Co_9S_8	**0.5 M**	**0.56**	**-86**	**115.9**	**This work**

Table S2. The BET of pristine Co_9S_8 and Co^{2+}-Co_9S_8 samples.

Samples	BET Surface Area $(m^2 \cdot g^{-1})$	Pore Volume $(cm^3 \cdot g^{-1})$
Co_9S_8	55.4	0.06
Co^{2+}-Co_9S_8	43.4	0.22

Table S3. The calculated absorption energy for H and Gibbs free-energy for HER based on the pure Co_9S_8 and Co^{2+}-Co_9S_8 systems

Samples	ΔE_H (eV)	ΔG_H (eV)
Co_9S_8	0.12	0.36
Co^{2+}-Co_9S_8	-0.48	-0.24

References

[S1] L. Wang, X. Duan, X. Liu, J. Gu, R. Si, Y. Qiu, Y. Qiu, D. Shi, F. Chen, X. Sun, *Adv. Energy Mater.* **2020**, *10*, 1903137.

[S2] H. Zhu, J. Zhang, R. Yanzhang, M. Du, Q. Wang, G. Gao, J. Wu, G. Wu, M. Zhang, B. Liu, *Adv. Mater.* **2015**, *27*, 4752-4759.

[S3] L. Wang, X. Wu, S. Guo, M. Han, Y. Zhou, Y. Sun, H. Huang, Y. Liu, Z. Kang, *J. Mater. Chem. A* **2017**, *5*, 2717-2723.

[S4] S. Peng, L. Li, X. Han, W. Sun, M. Srinivasan, S. G. Mhaisalkar, F. Cheng, Q. Yan, J. Chen, S. Ramakrishna, *Angew. Chem. Int. Ed.* **2014**, *126*, 12802-12807.

[S5] Y. Yang, H. Yao, Z. Yu, S. M. Islam, H. He, M. Yuan, Y. Yue, K. Xu, W. Hao, G. Sun, *J. Am. Chem. Soc.* **2019**, *141*, 10417-10430.

[S6] H. Li, X. Qian, C. Xu, S. Huang, C. Zhu, X. Jiang, L. Shao, L. Hou, *ACS Appl. Mater. Interf.* **2017**, *9*, 28394-28405.

[S7] H. Meng, W. Zhang, Z. Ma, F. Zhang, B. Tang, J. Li, X. Wang, *ACS Appl. Mater. Interf.* **2018**, *10*, 2430-2441.

[S8] H. Lv, Z. Xi, Z. Chen, S. Guo, Y. Yu, W. Zhu, Q. Li, X. Zhang, M. Pan, G. Lu, *J. Am. Chem. Soc.* **2015**, *137*, 5859-5862.

[S9] H. Wang, S. Min, Q. Wang, D. Li, G. Casillas, C. Ma, Y. Li, Z. Liu, L.-J. Li, J. Yuan, *ACS nano* **2017**, *11*, 4358-4364.

[S10]   X. Huang, X. Xu, C. Li, D. Wu, D. Cheng, D. Cao, *Adv. Energy Mater.* **2019**, *9*, 1803970.